Appl Nanosci (2015) 5:983–991
DOI 10.1007/s13204-014-0396-0

ORIGINAL ARTICLE

Electrochemical synthesis, characterisation and phytogenic properties of silver nanoparticles

R. Singaravelan · S. Bangaru Sudarsan Alwar

Received: 11 December 2014 / Accepted: 22 December 2014 / Published online: 18 January 2015

Abstract This work exemplifies a simple and rapid method for the synthesis of silver nanodendrite with a novel electrochemical technique. The antibacterial activity of these silver nanoparticles (Ag NPs) against pathogenic bacteria was investigated along with the routine study of optical and spectral characterisation. The optical properties of the silver nanoparticles were characterised by diffuse reflectance spectroscopy. The optical band gap energy of the electrodeposited Ag NPs was determined from the diffuse reflectance using Kubelka–Munk formula. X-ray diffraction (XRD) studies were carried out to determine the crystalline nature of the silver nanoparticles which confirmed the formation of silver nanocrystals. The XRD pattern revealed that the electrodeposited Ag NPs were in the cubic geometry with dendrite preponderance. The average particle size and the peak broadening were deliberated using Debye–Scherrer equation and lattice strain due to the peak broadening was studied using Williamson–Hall method. Surface morphology of the Ag NPs was characterised by high-resolution scanning electron microscope and the results showed the high degree of aggregation in the particles. The antibacterial activity of the Ag NPs was evaluated and showed unprecedented level antibacterial activity against multidrug resistant strains such as Staphylococcus aureus, Bacillus subtilis, Klebsiella pneumonia and Escherichia coli in combination with Streptomycin.

Keywords Antibacterial activity · Silver nanodendrite · UV-DRS · Williamson–Hall method · Kubelka–Munk plot

R. Singaravelan (✉) · S. Bangaru Sudarsan Alwar
Post Graduate and Research Department of Chemistry, D. G. Vaishnav College, Chennai, India
e-mail: shivramki31@gmail.com

Introduction

Nanoparticle research has become an immense developing field due to its wide range of applications in different areas of science and technology. Nanomaterials are gaining interest and prominence due to their many new-fangled properties in contrast to that in traditional bulk materials. Among the metal nanoparticles (NPs), transition metal NPs, in particular the nanoparticles of cobalt (Farhadi and Safabakhsh 2013), nickel (Abdelhalim et al. 2012; Huang et al. 2007 Au, He et al. 2013; Nejati and Zabihi 2012; Wang et al. 2008), palladium (Xiong et al. 2005; Jana et al. 2000); platinum (Roldan Cuenya et al. 2011; Zhang et al. 2008), gold (Merza1 et al. 2012) and titanium (Mishra et al. 2010), have attracted much attention of the researchers for a long time due to their size-induced properties and application-oriented importance in many industries as well as in advanced technologies. Among these transition metal nanoparticles, silver nanoparticles (Ag NPs) have been extensively studied due to their surface enhanced properties with fascinating structures and unique electrical, chemical, optical and antimicrobial properties.

For the past few decades, nanoparticles of silver have been gaining much attention and being used in almost every field, including medicine (Nithya and Ragunathan 2014; Knetsch and Koole 2011), catalysis (Venkatesham et al. 2012), bio sensing (Priyanka et al. 2013; Doria et al. 2012; Zhu et al. 2009), drug delivery (Soumya and Gayatri Hela 2013; Prabhu and Uzzaman 2011; Diaz and Vivas-Mejia 2013), electronics (Zhang et al. 2011; Lu 2007; Karni et al. 2012), textile (Xue et al. 2012), photonics (Shen et al. 2000), optical sensor (Pandey et al. 2012), non-linear optical properties (Ye et al. 2009; Vasireddy and Paul 2012), water treatment (Monyatsi et al. 2012; Ebeling et al. 2013), pigments, photographic, bactericide (Kim

et al. 2007; Govarthanan et al. 2014; Rajawat and Qureshi 2012; Li et al. 2013; Yasina et al. 2013), anticancer agent (Devi and Bhimba 2012; Mukherjee et al. 2014; Sulaiman et al. 2013; Nazir et al. 2011), wound treatment (Habiboallah et al. 2014), conductive composites (Pandey et al. 2012), etc.

Silver nanoparticles show a sharp and distinct optical response (surface plasmon resonance) in the visible region, which makes them potentially useful in optical biosensors and optoelectronic devices. The optical properties of the silver NPs have already been established in optoelectronic devices. And most significantly the Ag NPs are finding application in the field of medicine as an antibacterial agent and a therapeutic agent. In particular, the Ag NP bactericidal application is among the most studied in nanoscience. Silver nanoparticles provide a large number of active surfaces for their antibacterial interactions which make them interesting for biological and medical applications.

Medicinal and preservative properties of silver have been known for over 2,000 years. Since ancient times silver has been highly regarded as a versatile healing tool and been revered by the medical community; Hippocrates, the father of medicine knew its healing and anti-disease properties. Before the advent of antibiotics, silver was an important weapon against diseases. The ancient Phoenicians knew enough to keep water, wine and vinegar in silver vessels to ensure freshness. It was proved that silver dissolves in water forming a colloidal solution that kills pathogenic bacteria. And although the stability of silver in water is low, it is quite enough for disinfection. It is well known that silver nanoparticles are exceedingly toxic to microorganisms showing strong biocidal effects on Gram positive, Gram negative and fungous. There have already been developed several applications such as water filtering, food packing, silver nanoparticle-based antiseptics and anti-stain clothes (Vankar and Shukla 2012), which use the bactericidal effect of silver nanoparticles.

Nanoparticles are generally synthesised by physical (top-down), chemical and biological (bottom-up) methods. Owing to the wide range of applications offered by nanoparticles in various fields, different approaches have been deliberated for their synthesis. Several methodologies were developed to obtain Ag NPs of wide ranging surface morphology including, biosynthesis (Vankar and Shukla 2012; Christensen et al. 2011, Shanmugavadivu et al. 2014), microwave processing (Pal et al. 2013), laser ablation (Amendola et al. 2012), gamma irradiation (Gasaymeh et al. 2010), electron irradiation (Misra et al. 2013), electrodeposition (Khaydarov et al. 2008; Sanchez et al. 2000; Roldan et al. 2013), green synthesis (Shameli et al. 2012; Pandey et al. 2012; Ahmad and Sharma 2012), sonoelectrochemical synthesis (Socol et al. 2002); chemical reduction (Sileikaite et al. 2009), photochemical method (Kutsenko and Granchak 2009), thermal decomposition, radiolytic reduction (Saion et al. 2013) etc., Among these techniques, bottom-up methods are frequently adopted for the synthesis of Ag NPs, since they offer easy and expedient route for the synthesis of Ag NPs.

Among them electrochemical method is the most popular and frequently used method for the Ag NPs synthesis. An inexpensive conventional two-electrode system was used for the electrochemical synthesis. The advantage of this technique over other bottom-up approaches lies in the purity of the nanoparticles. Since the method is flexible, the particle size can be improved by controlling the reaction parameters such as electrolytic concentration and the applied current density. This technique employs the use of inexpensive chemicals and materials for the Ag NPs synthesis. However, there were no special reagents like surfactants and reducing agents were used in the present work for the stability and reduction of silver ion in solution.

Experimental

Materials and method

Analytical grade silver nitrate ($AgNO_3$) was obtained from M-Merck and used without further purification. High-grade glassy carbon rod from Alfa Aesar was used as the counter electrode and silver metal (99.9 % pure) with geometric area of 20 mm × 2 mm × 30 mm was used as working electrode for the electrolysis. The electrolyte was prepared using double-distilled deionized water and both the electrodes were immersed in the electrolyte and held parallel to each other at the distance of 2 cm. The Ag ion reduction in the electrolysis process was carried out by inducing a chemical reaction in an electrolyte by the applied voltage across the electrodes. Regulated power supply battery unit was used as the direct current (DC) source for the electrolysis process and the constant current was drawn at the rate of 10 mA per second throughout the process. The electrochemical process was carried out at room temperature and the pH of the electrolyte was not maintained but then it was observed that the pH of the electrolyte was decreasing as the deposition progresses.

Electrochemical synthesis of silver nanoparticles

Electrochemical deposition is a technique that has been widely used for the synthesis of metal nanoparticles. Electrochemical deposition occurs at the interface of an electrolyte solution containing the metal to be deposited and an electrically conductive metal substrate. Silver nanoparticles were synthesised electrochemically using an electrolyte containing 0.01 mM concentration of $AgNO_3$.

The electrolyte was prepared from double deionised water and the volume of the cell was 100 ml. The glassy carbon electrode and the silver metal were employed as working electrode and counter electrodes, respectively. Ag NPs showed dendritic growth and it was found that high concentration of the silver ion favours the aggregation and dendritic formation. The overall cathodic reduction of silver ions at room temperature can occur in the following way.

$$Ag^{+}_{aq} + e^{-} \rightarrow Ag.$$

Characterisation

The formation of Ag NPs was confirmed by X-ray diffraction technique using diffractometer with Cu-Kα radiation ($\lambda = 1.5406$ Å). Particle size and anisotropic nature of the Ag NPs were calculated using Scherrer formula and Williamson–Hall equation. Diffuse reflectance spectroscopy (DRS) was used to characterise the optical properties of the Ag NPs. Scanning Electron Microscopy was used to determine the size and morphology of the Ag NPs obtained from electrodeposition method.

Antibacterial assay

The high chemical reactivity of silver ions allows the silver surface to enter the strong bonds with groups containing carbon monoxide, carbon dioxide, or oxygen, which then leads to the prevention of bacteria/fungi spreading. There are number of techniques available to perform antibacterial and antimicrobial susceptibility tests which include agar disc diffusion (Kirby–Bauer), broth diffusion (Stokes) (macro- and micro-dilution), agar dilution (minimum inhibitory concentration) and diffusion and dilution (*E* test) method. The antimicrobial susceptibility of silver nanoparticles was evaluated for both Gram-positive and Gram-negative bacteria using the Kirby–Bauer disc diffusion method. Kirby–Bauer method is most commonly used for antibacterial investigation since the method being recommended by the National Committee for Clinical Laboratory Standards (NCCLS). The zone of inhibition was measured after 24 h of incubation at room temperature.

Results and discussions

UV-DRS

UV-diffuse reflectance spectroscopy is one of the most widely used techniques for structural characterisation of the metal nanoparticles. Due to the unique optical properties of the Ag NPs, great deal of information about the physical state of the nanoparticles can be obtained by analysing the optical characterisation of Ag NPs. It is known that the size and shape of the Ag NPs considerably change their optical properties since the surface-to-volume ratio increases with decrease in size of the particle. Ultraviolet–visible spectroscopy of the silver nanocrystals was performed in a Perkin Elmer Lamda-2 spectrophotometer and is shown in Fig. 1. The surface plasmon resonance band was detected for a primary peak around 398 nm which indicates the cluster formation and a secondary peak at 339 nm confirms that the Ag NPs are dendritic in nature.

Peak position and sharp intensity of the absorption spectrum revealed the presence of Ag NDs and it was confirmed by the SEM results of the Ag NPs. The shapes of the absorption curve suggest that the nanoparticles were well dispersed and spherical in shape. Since the cluster formation is seen, the absorption is observed towards the blueshift. The stability of the Ag NDs was confirmed by observing the absorption spectrum after 30 days of synthesis.

According to Mie theory, spherical Ag NPs exhibit single surface plasmon band, while dispersed anisotropic particles such as dendrites, prism, rod and triangles exhibit two or three SPR bands. At diameters greater than 10 nm, a second peak becomes visible at a shorter wavelength than the primary peak. This secondary peak is due to a quadruple resonance that has a different electron oscillation pattern than the primary dipole resonance. When Ag NPs aggregate, the metal particle becomes electrically coupled and this system has different SPR than the individual particles and it is shifted to longer wavelength. As the diameter increases, the plasmon resonance peak shifts to longer wavelengths and broadens. The absorption spectrum of the Ag NPs showed a surface plasmon resonance peak which indicates that the Ag NPs are dendrites with small

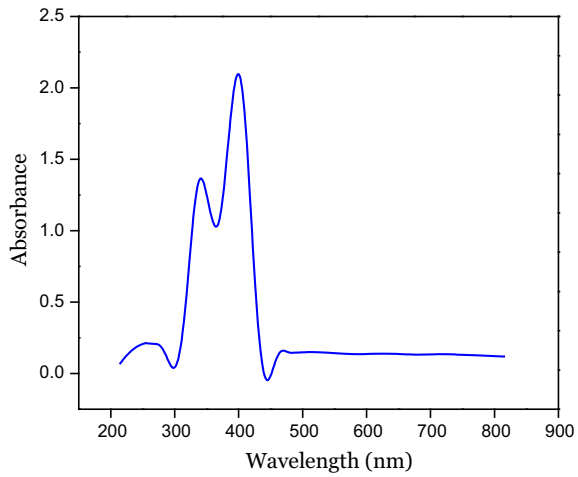

Fig. 1 UV-DRS spectrum for the Ag NPs

particle size and are not aggregated to the large particles and is confirmed by the HR-SEM images.

Band gap energy

Band gap is the major factor determining the electrical conductivity of a solid. Substances with large band gap are generally insulators (dielectric), those with smaller band gaps are semiconductors, while conductors either have very small band gap or no band gap because the valence and conduction bands overlap. The band gap is the minimum amount of energy required for an electron to break free of its bound state. Electrons with enough thermal energy can jump from the valence band to conduction band.

Kubelka–Munk method

The strong interaction of Ag NPs with visible light occurs because the conduction electrons on the metal surface undergo a collective oscillation when excited by light at specific wavelength. The optical band gap energy for the Ag NDs was calculated using Tauc equation as follows:

$$(\alpha h\nu)^n = A\left(h\nu - E_g\right), \tag{1}$$

where A is a constant, α the absorption coefficient, E_g. is the band gap, h is the planck's constant, ν. is the frequency, and n equals to ½ for the allowed direct transition.

The absorption coefficient value is calculated from the diffuse reflectance using Kubelka–Munk equation,

$$\mathrm{F}(R) = \frac{(1-R)^2}{2R} = \frac{k}{s}, \tag{2}$$

where, R is the absolute reflectance of the Ag NPs, k the molar absorption coefficient and s the scattering coefficient. The acquired diffuse reflectance spectrum is converted to Kubelka–Munk function F(R), which is equivalent to the absorption coefficient (α). Thus the vertical axis is converted into the quantity $[\mathrm{F}(R)h\nu]^{0.5}$. and plotted against photon energy $(h\nu)$. The band gap value is obtained by the intercept of the fitted straight line of the linear part of the curve. The value of optical band gap energy for the electrodeposited As was found to be 3.37 eV and is shown in the Fig. 2.

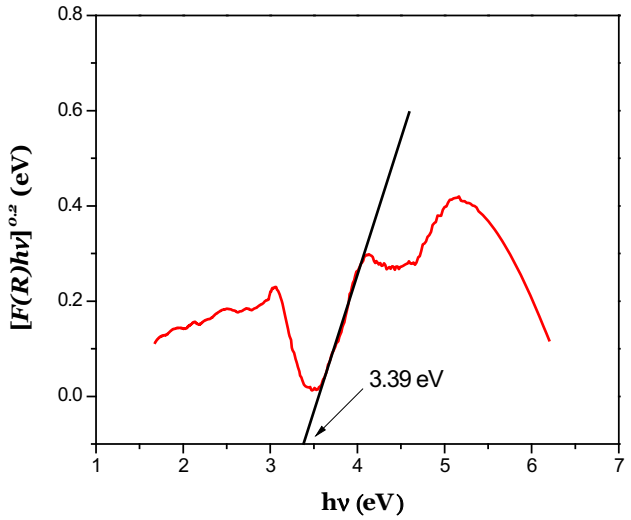

Fig. 2 Kubelka–Munk Plot for band gap calculation

HR-SEM

Structural morphology of Ag NPs was characterised by FEI Quanta FEG 200 electron microscope. Figure 3 shows the HR-SEM images of the well-dispersed Ag NDs synthesised at room temperature. HR-SEM results showed that the Ag NPs obtained by the electrochemical synthesis are pure in nature and dendritic in shape, with the size 10–50 nm and are in good agreement with the XRD analysis.

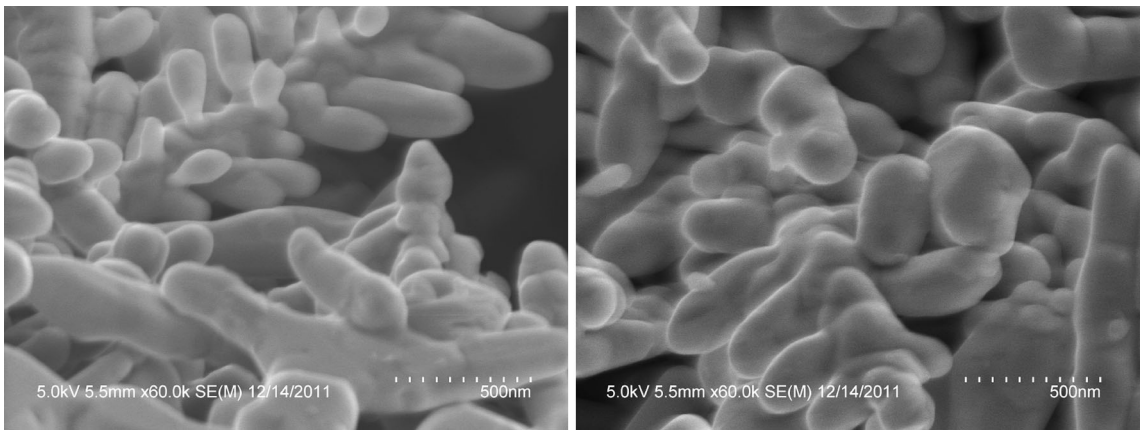

Fig. 3 FE-SEM micrographs of Ag NDs

X-ray diffraction analysis

The crystalline structure of the synthesised Ag NPs was investigated through powder X-ray diffraction by a Seifert Analyse X-ray powder diffractometer using Cu Kα radiation operating between 10° and 70° and is shown in Fig. 4. XRD analysis showed that, Ag NPs are highly crystalline in nature and have face-centred (FCC) geometry. The XRD pattern showed diffraction peaks at 2θ values of 38.16°, 44.35°, and 64.47° corresponding to (111), (200), and (220) Bragg's reflections, respectively. The XRD pattern exhibited higher preferential orientation at $2\theta = 38.16°$ corresponding to (111) reflection of the Ag NDs. This was in good agreement with the unit cell of the face-centred cubic (fcc) structures (JCPDS file no. 04-0783) with a lattice parameter of $a = 4.077$ Å.

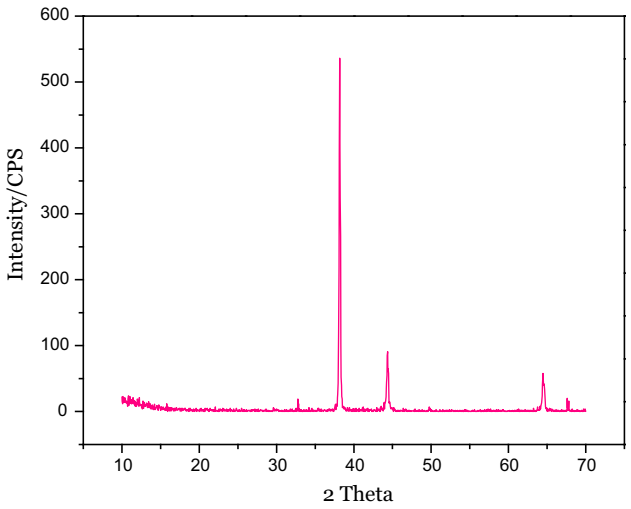

Fig. 4 XRD pattern of the electrodeposited Ag NPs

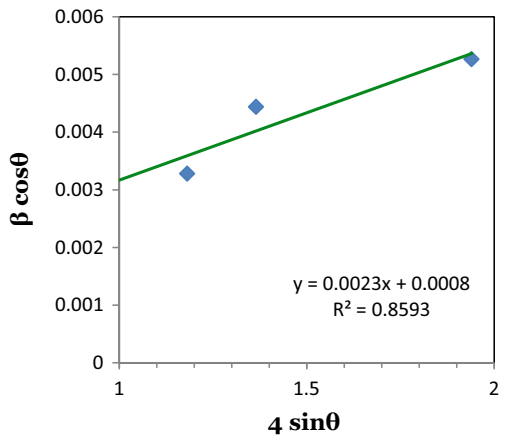

Fig. 5 Williamson–Hall analysis of silver nanodendrites. Fit to the data, strain is determined from the slope and crystalline size from the intercept of the fit

Particle size and strain

The crystalline size of the synthesised Ag Np was calculated using peak broadening method using Debye–Scherrer formula and the average crystalline size is found to be 33.3 nm.

$$D = \frac{K\lambda}{\beta_{hkl}\mathrm{Cos}\theta}, \tag{3}$$

where D is the grain size (nm), λ the wavelength of X-ray used (nm), θ the diffraction angle (degrees), K is a constant equal to 0.94, β the peak width at full width half maximum (FWHM) of X-ray diffraction peak (rad.). The X-ray diffraction pattern nanocrystalline silver exhibited significant line broadening.

Average crystalline size and strain-induced broadening due to crystal imperfection and distortion were calculated using Williamson–Hall formula,

$$\beta_{hkl}\cos\theta = \frac{K\lambda}{D} + 4\varepsilon\sin\theta. \tag{4}$$

A plot is drawn with $4\sin\theta$. along the x-axis and $\beta_{hkl}\cos\theta$. along the y-axis as shown in Fig. 5. From the linear fit to the data, the crystalline size was calculated from the ordinate intercept, and the strain from the slope of the fit. The geometrical parameters of the Ag NPs are summarised in Table 1.

FT-IR spectrum

An infrared study was carried out to establish the purity and nature of the silver nanoparticles obtained from the electrodeposition method. The FT-IR spectrum obtained for Ag NPs shows different absorption peaks and is shown in Fig. 6. A strong absorption observed at 3,452 cm^{-1} was

Table 1 X-ray diffraction geometrical parameters of Ag NPs

d-spacing (Å)	2θ position	hkl	β-radians	Lattice parameter (a) Å	Relative int. (%)	Particle size (nm)	
						Scherrer method	W–H method
2.3559	38.1695	111	3.43×10^{-3}	4.0804	100	42.32	42
2.0405	44.3575	200	4.72×10^{-3}	4.0810	22	31.27	
1.4440	64.4786	220	6.02×10^{-3}	4.0842	17	26.34	

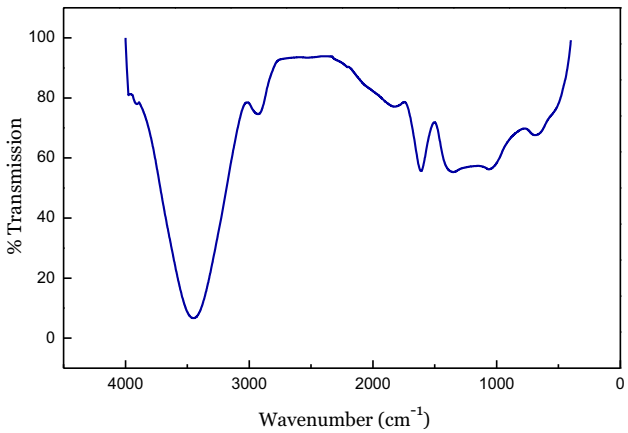

Fig. 6 FTIR spectrum of the Ag NDs

due to the O–H stretching vibration of water molecule adsorption on the metal surface. A sharp band observed at 1,621 cm^{-1} and a weak absorption at 687 cm^{-1} can be attributed to symmetric stretching vibration of N = O bond of NO_2 ion which could be from the $AgNO_3$. electrolyte. Very weak absorption peaks at 1,354 cm^{-1} indicate the in-plane bending mode of water molecule on the surface of the Ag NPs.

Antibacterial susceptibility

Ag NPs specifically have been proven to have effective antiviral qualities and their toxicity to a wide range of microorganisms is dependent on a variety of qualities. The small size of the Ag NPs allows them to interact with the

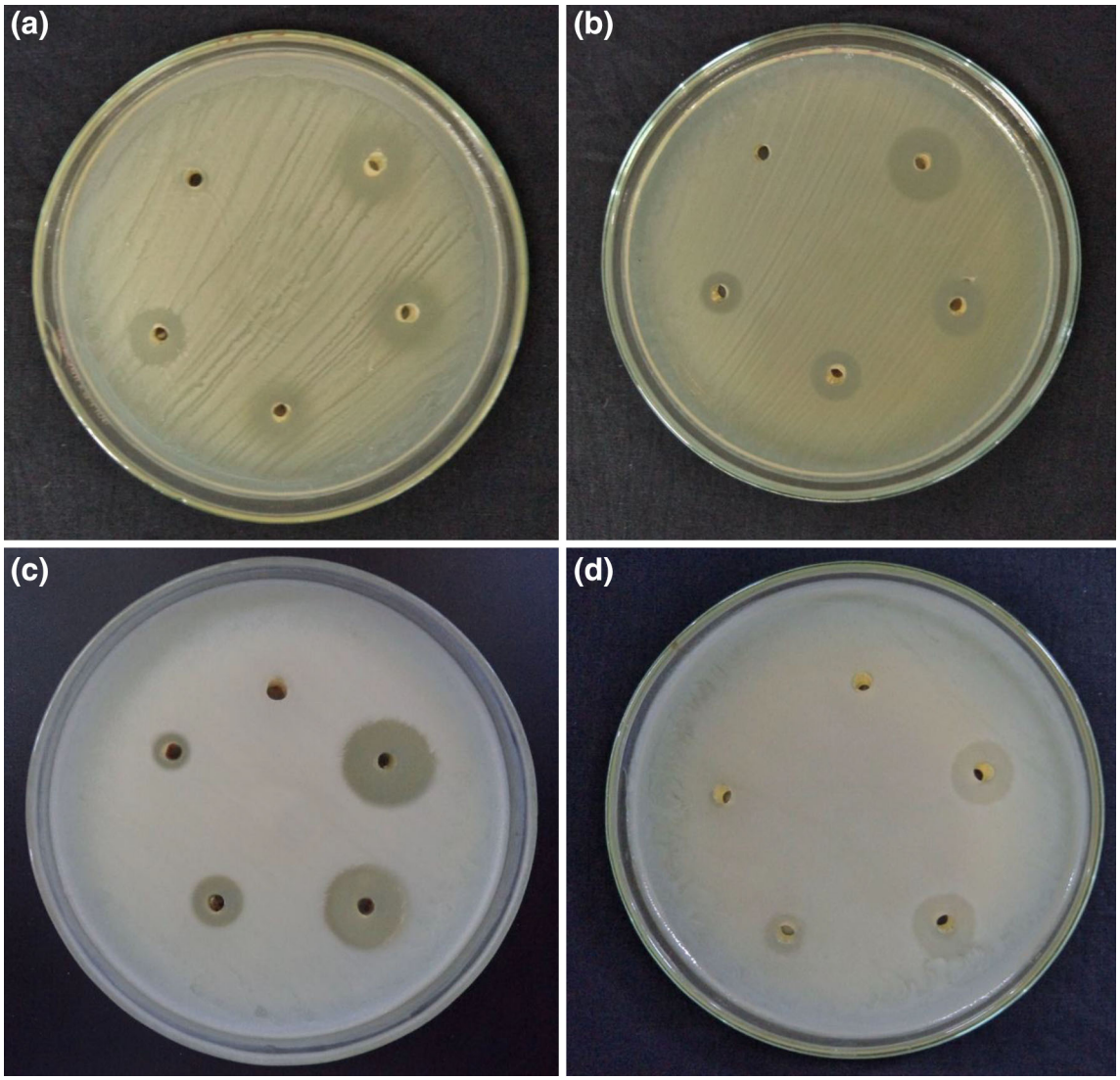

Fig. 7 Zone of inhibition disc impregnated with Ag NPs at different concentrations of (30, 40 and 50) against (**a**) *Klebsiella pneumonia*, (**b**) *Escherichia coli*, (**c**) *Bacillus subtilis* and (**d**) *Staphylococcus aureus*

membranes of bacteria and viruses by their ability to cross the membranes of both Gram-positive and Gram-negative bacteria. Ag ions cause destruction of the peptidoglycan bacterial cell wall and lysis of the cell membrane. Ag ions may denature ribosomes thereby inhibiting protein synthesis and causing degradation of the plasma membrane. Silver ions bind to DNA bases causing DNA to condense and lose its ability to replicate, thereby preventing bacterial reproduction via binary fusion. Silver interrupts the bacteria cell's ability to form chemical bonds essential for their survival. These bonds produce the cell's physical structure so that when bacteria meets Ag it literally falls apart.

The actual mechanism for the bactericidal effect has not been completely unravelled. However, the possible bactericidal mechanism for Ag NPs may be

1. Cell uptake followed by disruption of both ATP production and DNA replication.
2. Cell membrane damage.
3. Generation of reactive oxygen species.

Methicillin-resistant Staphylococcus aureus (MRSA), a life-threatening Steph often referred to as a "Super bug" is resistant to almost all chemical antibiotics. Silver nanoparticles have been proven to have better bactericidal effect and biofilm formation on Staphylococcus aureus (MRSA).

Silver has actually been proven to promote the growth of new cells, thereby increasing the rate at which wounds can heal. An added advantage is that unlike other metals with antibacterial properties, Ag is not toxic to humans.

It was proven that, silver nanoparticles (Ag NPs) can prevent photosynthesis in algae.

Many aspects of the inhibitory effect of Ag ion have been discussed previously. The antibacterial susceptibility of the electrodeposited Ag NPs was evaluated by Kirby–Bauer disc diffusion method using Muller-Hinton agar (MHA) medium. Zone of inhibition was measured after 24 h of incubation at room temperature. The bacterial growth was determined by measuring the diameter of inhibition zone and is shown in Fig. 7. Figure 8 explains the effect of Ag NPs concentration compared with the standard antibiotic Streptomycin. Ag NPs exhibited distinct antibacterial activity against Gram-positive and Gram-negative bacteria. The minimum inhibitory concentrations (MIC) of Ag NPs against the bacterial strain are given in Table 2. The synergetic effect of Ag NPs along with the antibiotic drug Streptomycin (10 μg) was found to be effective.

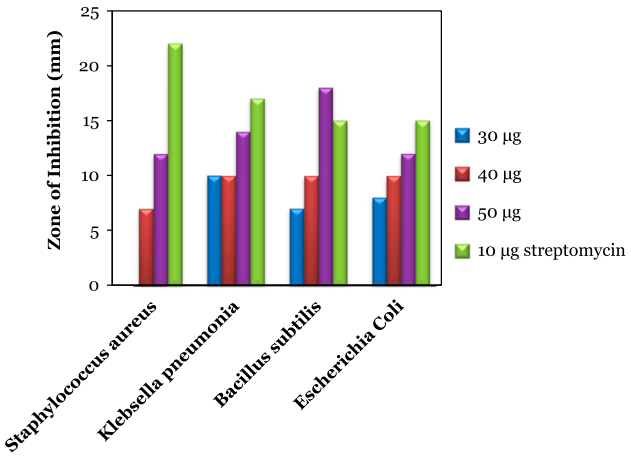

Fig. 8 The antibacterial effect of Ag NPs on gram positive and gram negative bacteria

Table 2 Zone of Inhibition

Bacteria	Zone of inhibition (mm)				
	Negative control	30 μg	40 μg	50 μg	Positive control
Staphylococcus aureus	0	0	7	12	15
Klebsiella pneumonia	0	10	10	12	15
Bacillus subtilis	0	7	10	18	22
Escherichia coli	0	8	10	12	17

Conclusion

A novel one-pot synthesis route for the qualitative synthesis of highly stable Ag NPs is reported without using any special reagent. This work summarises the novel technique for the synthesis of stable silver nanoparticles. Electron microscopy result confirmed the formation of Ag NPs and XRD results showed the high crystallinity of the electrodeposited Ag NDs. The FT-IR spectrum showed that the Ag NPs obtained are free from impurities. Ag ND formation was once again confirmed by UV–Vis characterisation and the surface plasmon resonance band of the Ag NPs with the optical band gap energy of 3.39 eV can be a potential candidate for the optical and optoelectronic devices. In addition, the antibacterial activity of the electrodeposited silver NPs was also evaluated and showed excellent bactericidal activity against both Gram-positive and Gram-negative bacteria. These results indicate that the Ag NPs can be used as an antibacterial agent in the field of medicine. At higher concentration, the Ag NPs showed better bactericidal effect towards the Gram-positive bacteria compared to Gram-negative bacteria. The synergetic effect of Ag NPs was more pronounced on Gram-negative bacteria than on Gram-positive bacteria because the cell wall of the Gram-negative bacteria is thinner.

References

Abdelhalim MAK, Mady MM, Ghannam MM (2012) Physical properties of different gold nanoparticles: ultraviolet-visible and fluorescence measurements. J Nanomed Nanotechol 3:3

Ahmad N, Sharma S (2012) Green synthesis of silver nanoparticles using extracts of *Ananas comosus*. Gr Sustain Chem 2:141–147

Amendola V, Polizzi S, Meneghetti M (2012) Laser ablation synthesis of silver nanoparticles embedded in graphitic carbon matrix. Sci Adv Mater 4:1–4

Christensen L, Vivekanandhan S, Misra M, Mohanty A (2011) Biosynthesis of silver nanoparticles using murraya koenigii (curry leaf): an investigation on the effect of broth concentration in reduction mechanism and particle size. Adv Mat Lett 2(6):429–434

Devi JS, Bhimba BV (2012) Anticancer activity of silver nanoparticles synthesized by the seaweed *Ulva lactuca* Invitro. Open Access Sci Rep 4(1):242

Diaz MR, Vivas-Mejia PE (2013) Nanoparticles as drug delivery systems in cancer medicine: emphasis on RNAi-containing nanoliposomes. Pharmaceuticals 6:1361–1380

Doria G, Conde J, Veigas B, Giestas L, Almeida C, Assuncao M, Rosa J, Baptista PV (2012) Sensors 12:1657–1687

Ebeling A, Hartmann V, Rockman A, Armstrong A, Balza R, Erbe J, Ebeling D (2013) Silver nanoparticle adsorption to soil and water treatment residuals and impact on Zebrafish in a Lab-scale constructed Wetland. Comput Water, Energy, Environ Eng 2:16–25

Farhadi S, Safabakhsh J, Zaringhadam P (2013) Synthesis, characterisation, and investigation of optical and magnetic properties of cobalt oxide (Co_3O_4) nanoparticles. J Nan Chem 3:69

Gasaymeh SS, Radiman S, Heng LY, Saion E, Saeed GHM (2010) Synthesis and characterization of silver/polyvinilpirrolidone (Ag/PVP) nanoparticles using gamma irradiation techniques. Am J Appl Sci 7(7):892–901

Govarthanan M, Selvankumar T, Manoharan K, Rathika R, Shanthi K, lee K-J, Cho M, Kamala-Kannan S (2014) Biosynthesis and characterization of silver nanoparticles using panchakavya, an Indian traditional farming formulating agent. Int J Nanomed 9:1593–1599

Habiboallah G, Mahdi Z, Majid Z, Nasroallah S, Taghavi AM, Forouzanfar A, Arjmand N (2014) Enhancement of gingival wound healing by local application of silver nanoparticles periodontal dressing following surgery: a histological assessment in animal model. Mod Res Inflamm 3:128–138

He X, Zhong W, Au CT, Du Y (2013) Size dependence of the magnetic properties of Ni nanoparticles prepared by thermal decomposition method. Nanoscale Res Lett 8:446

Huang X, Jain PK, El-sayed IH, El-sayed MA (2007) Gold nanoparticles: interesting optical properties and recent applications in cancer diagnostics and therapy. Nanomedicine 2(5):681–693

Jana NR, Wang ZL, Pal T (2000) Redox catalytic properties of palladium nanoparticles: surfactant and electron donor–acceptor effects. Langmuir 16:2457–2463

Karni TC, Langer R, Kohane DS (2012) The smartest materials: the future of nanoelectronics in medicine. ACS Nano 6:6541–6545

Khaydarov RA, Khaydarov RR, Gapurova O, Estrin Y, Scheper T (2009) Electrochemical method for the synthesis of silver nanoparticles. J Nanopart Res 11:1193–1200

Kim JS, Kuk E, Yu KN, Kim J, Park SJ, Lee HJ, Kim SH, Park YK, Park YH, Hwang CY, Kim YK, Lee YS, Jeong DH, Cho MH (2007) Antimicrobial effects of silver nanoparticles. Nanomedicine: nanotechnology. Biol Med 3:95–101

Knetsch MLW, Koole LH (2011) New strategies in the development of antimicrobial coatings: the example of increasing usage of silver and silver nanoparticles. Polymers 3:340–366

Kutsenko AS, Granchak VM (2009) Photochemical synthesis of silver nanoparticles in polyvinyl alcohol matrices. Theor Exp Chem 45:313–318

Li WC, Volodymyr K, Wang Y, Volodymyr D (2013) The bactericidal spectrum and virucidal effects of silver nanoparticles against the pathogens in sericulture. Open J Anim Sci 3:169–173

Lu W (2007) Lieber CM: nanoelectronics from the bottom up. Nat Mater 6:841–850

Merza Khalida S, Al-Attabi Hadi D, Abbas Zaid M, Yusr Hashim A (2012) Comparative study on methods for preparation of gold nanoparticles. Gr Sustain Chem 2:26–28

Mishra S, Gupta SK, Jha PK, Pratap A (2010) Study of dimension dependent diffusion coefficient of titanium dioxide nanoparticles. Mater Chem Phys 123:791–794

Misra N, Biswal J, Dhamgaye VP, Lodha GS, Sabharwal S (2013) A comparative study of gamma, electron beam, and synchrotron X-ray irradiation method for synthesis of silver nanoparticles in PVP. Adv Mat Lett 4(6):458–463

Monyatsi LM, Mthombeni NH, Onyango MS, Momba MNB (2012) Cost-effective filter materials coated with silver nanoparticles for the removal of pathogenic bacteria in groundwater. Int J Environ Res Public Health 9:244–271

Mukherjee S, Chowdhury D, Kotcherlakota R, Patra S, Vinothkumar B, Bhadra MP, Sreedhar B, Patra CR (2014) Potential theranostics application of bio-synthesized silver nanoparticles (4-in-1 system). Theranostics 4(3):316–335

Nazir S, Hussain T, Iqbal Md, Mazhar K, Muazzam AG, Ismail J Md (2011) Novel and cost-effective green synthesis of silver nano particles and their in vivo antitumor properties against human cancer cell lines. Biosci Tech, 2 (6), 425–430

Nejati K, Zabihi R (2012) Preparation and magnetic properties of nano size nickel ferrite particles using hydrothermal method. Chem Cent J 6:23

Nithya R, Ragunathan R (2014) In vitro synthesis, characterization and medical application of silver nanoparticle by using a lower fungi. Middle-East J Sci Res 21(6):922–928

Pal J, Deb MK, Deshmukh D (2014) Microwave-assisted synthesis of silver nanoparticles using benzo-18-crown-6 as reducing and stabilizing agent. Appl Nanosci 4:507–510

Pandey S, Goswami GK, Nanda KK (2012) Green synthesis of biopolymer–silver nanoparticles nanocomposite: an optical sensor for ammonia detection. Int J Biol Macromol 51:583–589

Prabhu V, Uzzaman S, Berlin Grace VM, Guruvayoorappan C (2011) Nanoparticles in drug delivery and cancer therapy: the giant rats tail. J Cancer Ther 2:325–334

Priyanka S, Shashank P, Muhammad Aslam MK, Prashant S, Krishan Pa S (2013) Nanobiosensors: diagnostic tool for pathogen detection. Int Res J Biological Sci 2(10):76–84

Rajawat S, Qureshi MS (2012) Comparative study on bactericidal effect of silver nanoparticles, synthesized using green technology, in combination with antibiotics on *Salmonella typhi*. J Biomat Nanobiotech 3:480–485

Roldan Cuenya B, Ortigoza MA, Ono LK, Behafarid F, Mostafa S, Croy JR, Paredis K, Shafai G, Rahman TS, Li L, Zhang Z, Yang JC (2011) Thermodynamic properties of Pt nanoparticles: size, shape, support, and adsorbate effects. Phys Rev 84:245438

Roldan MV, Pellegri N, Oscar de Sanctis (2013) Electrochemical method for Ag-PEG nanoparticles synthesis. J Nanopart 524150

Saion E, Gharibshahi E, Naghavi K (2013) Size-controlled and optical properties of monodispersed silver nanoparticles synthesized by the radiolytic reduction method. Int J Mol Sci 14:7880–7896

Sanchez LR, Blanco MC, Lopez-Quintela MA (2000) Electrochemical synthesis of silver nanoparticles. J Phys Chem B 104:9683–9688

Shameli K, Ahmad Mansor, Jazayeri SD, Shabanzadeh P, Sangpour P, Jahangirian H, Gharayebi Y (2012) Investigation of antibacterial properties of silver nanoparticles prepared via green method. Chem Cent J 6:73

Shanmugavadivu M, Kuppusamy S, Ranjithkumar R (2014) Synthesis of pomegranate peel extract mediated silver nanoparticles and its antibacterial activity. Am J Adv Drug Deliv 2(2):174–182

Shen Y, Friend CS, Jiang Y, Jakubczyk D, Swiatkiewicz J, Prasad PN (2000) Nanophotonics: interactions, materials, and applications. J Phys Chem B 104:7577–7587

Sileikaite A, Pusio J, Prosycevasi I, Tamulevicius S (2009) Investigation of silver nanoparticles formation kinetics during reduction of silver nitrate with sodium citrate. Mater Sci 15:1

Socol Y, Abramson O, Gedanken A, Meshorer Y, Berenstein L, Zaban A (2002) Suspensive electrode formation in pulsed sonoelectrochemical synthesis of silver nanoparticles. Langmuir 18:4736–4740

Soumya RS, Gayatri Hela P (2013) Nano silver based targeted drug delivery for treatment of cancer. Der Pharmacia Lettre 5(4):189–197

Sulaiman GM, Mohammed WH, Marzoog TR, Al-Amiery AAA, Kadhum AAH, Mohamad AB (2013) Green synthesis, antimicrobial and cytotoxic effects of silver nanoparticles using Eucalyptus chapmaniana leaves extract. Asian Pac J Trop Biomed 3(1):58–63

Vankar PS, Shukla D (2012) Biosynthesis of silver nanoparticles using lemon leaves extract and its application for antimicrobial finish on fabric. Appl Nanosci 2:163–168

Vasireddy R, Paul R, Mitra AK (2012) Green synthesis of silver nanoparticles and the study of optical properties. Nanomater Nanotechnol 2:8

Venkatesham M, Ayodhya D, Madhusudhan A, Veera Babu N, Veerabhadram G (2014) A novel green one-step synthesis of silver nanoparticles using chitosan: catalytic activity and antimicrobial studies. Appl Nanosci 4:113–119

Wang H, Kou X, Zhang J, Li J (2008) Large scale synthesis and characterization of Ni nanoparticles by solution reduction method. Bull Mater Sci 31(1):97–100

Xiong Y, Chen J, Wiley B, Xia Y, Yin Y, Li ZY (2005) Size-dependence of surface plasmon resonance and oxidation for pd nanocubes synthesized via a seed etching process. Nano Lett 5(7):1237–1242

Xue CH, Chen J, Yin W, Jia ST, Ma JZ (2012) Superhydrophobic conductive textiles with antibacterial property by coating fibers with silver nanoparticles. Appl Surf Sci 258:2468–2472

Yasina S, Liua L, Yao J (2013) Biosynthesis of silver nanoparticles by bamboo leaves extract and their antimicrobial activity. J. of Fiber Bioeng. and Inf. 6(1):77–84

Ye W, Shen C, Tian J, Wang C, Hui C, Gao H (2009) Controllable growth of silver nanostructures by a simple replacement reaction and their SERS studies. Solid State Sci 11:1088–1093

Zhang L, Fang Z, Zhao GC, Wei XW (2008) Electrodeposited platinum nanoparticles on the multi-walled carbon nanotubes and its electrocatalytic for nitric oxide. Int J Electrochem Sci 3:746–754

Zhang Z, Zhang X, Xin Z, Deng M, Wen Y, Song Y (2011) Synthesis of monodisperse silver nanoparticles for ink-jet printed flexible electronics. Nanotechnology 22:425601

Zhu S, Du C, Fu Y (2008) Fabrication and characterization of rhombic silver nanoparticles for biosensing. Opt Mater 31:769–774